pBOSC: A method for source-level identification of neural oscillations in electromagnetic brain signals

Authors

Enrique Stern[1], Guiomar Niso[2], Almudena Capilla[1]

Affiliation

[1] Departamento de Psicología Biológica y de la Salud, Facultad de Psicología. Universidad Autónoma de Madrid, Madrid, Spain.

[2] Cajal Institute & Cajal International Neuroscience Center, CSIC, Madrid, Spain

Corresponding Authors*: Enrique Stern, Almudena Capilla

Departamento de Psicología Biológica y de la Salud, Facultad de Psicología

Universidad Autónoma de Madrid

C/ Ivan Pavlov 6, 28049, Madrid, Spain

Phone number: +34 91 497 3383

E-mail: enrique.stern@uam.es; almudena.capilla@uam.es

Abstract

Neural oscillations are recognized as a fundamental component of brain electromagnetic activity. They are implicated in a wide range of cognitive processes and proposed as a core mechanism for brain communication. Nonetheless, detecting genuine neural oscillations remains a methodological challenge, particularly due to the difficulty of distinguishing them from aperiodic background activity. To identify episodes of oscillatory activity directly at their sources, we developed pBOSC, which extends the BOSC (Better OSCillation detection) family of algorithms. Consistent with existing approaches, pBOSC detects oscillatory episodes that exceed both a defined power threshold and a minimum duration criterion. In pBOSC, however, the detection of oscillatory episodes also relies on identifying peaks (i.e., local maxima) in the power spectra as well as throughout the brain volume. Using a series of simulated signals, we tested the ability of pBOSC to detect and localize oscillations across multiple scenarios. Our results show that most oscillatory episodes were accurately detected at their sources, achieving around 95% accuracy under optimal conditions (i.e., high signal-to-noise ratio, lower frequency, and longer oscillation duration). In addition, we validated pBOSC's performance on real resting-state magnetoencephalography (MEG) data. By extracting the natural frequency of each brain voxel from the detected oscillatory episodes, we observed a topographic distribution consistent with previous work. In conclusion, pBOSC offers a novel approach for identifying oscillatory activity in electrophysiological signals. It extends previous algorithms by operating in source space and verifying the presence of genuine spectral peaks, thereby enabling new possibilities for exploring brain dynamics.

1. Introduction

Neural oscillations have become a major area of interest in cognitive neuroscience, as different frequencies have been linked to a wide variety of cognitive processes and functions (Cannon et al., 2014; Helfrich et al., 2018; Herweg et al., 2020; Lega et al., 2012; Noah et al., 2020; Shin et al., 2017). Furthermore, several theoretical frameworks have posited brain oscillations as a fundamental mechanism for neural communication and temporal organization of brain function (Bonnefond et al., 2017; Buzsáki & Watson, 2012; Fries, 2015; Izhikevich et al., 2003; Palva & Palva, 2018; Vinck et al., 2023).

Nonetheless, studying neural oscillations constitutes a challenging task, since they are obscured by the so-called aperiodic component, a broadband signal that follows a power-law function, where power decreases exponentially with increasing frequency ($1/f^{\beta}$). This component is also referred to as arrhythmic, scale-free, pink noise, or background activity (He, 2014), indicating the lack of any characteristic frequency in the power spectrum. The aperiodic component has been suggested to reflect key physiological processes such as the balance between excitation and inhibition in neural circuits (Gao et al., 2017) and the population fire rate (He, 2014) and has been associated with task performance and various clinical conditions (Donoghue, 2024).

While most studies have traditionally relied on baseline subtraction to attenuate the aperiodic component (Gross, 2014; Gyurkovics et al., 2022), the idea of parameterizing the power spectrum to isolate oscillatory activity is rising in popularity (Donoghue et al., 2020). Thus, to confirm the presence of a neural oscillation, a narrow-band frequency peak must be detected over the aperiodic component (Donoghue et al., 2022; Gross, 2014; Lopes da Silva, 2013). Rhythmicity has also been proposed as a key feature of brain oscillations (Fransen et al., 2015), although this view is currently under debate, since oscillations do not always

manifest as sustained patterns, but often occur in the form of transient bursts (Jones, 2016; Van Ede et al., 2018; Vidaurre et al., 2016).

Despite its theoretical and methodological relevance, relatively few methods have been developed to detect episodes of oscillatory brain activity in electrophysiological data. A family of algorithms designed for this purpose is BOSC (Better OSCillation detection). A common practice across the different BOSC variants is to establish both a duration and a power threshold. The duration threshold is typically set at three consecutive cycles to minimize spurious results and guarantee rhythmicity. The definition of the power threshold has evolved with successive versions of the method. For example, in its original formulation (BOSC; Caplan et al., 2001; Whitten et al., 2011), a linear model of the aperiodic component was used to estimate the power threshold corresponding to the 95th percentile of a χ^2 distribution. The method was later extended (eBOSC; Kosciessa et al., 2020) and adapted to fit the model using robust regression, thus improving specificity of oscillatory activity detection. More recently, FOOOF (Fitting Oscillations and One-Over-F; (Donoghue et al., 2020), a popular spectral parameterization algorithm, has been incorporated within the BOSC framework to improve the estimation of the aperiodic component (fBOSC; Seymour et al., 2022). A related method outside the BOSC framework is PAPTO (Periodic/Aperiodic Parameterization of Transient Oscillations; Brady & Bardouille, 2022), which also uses FOOOF to model the aperiodic background and sets the power threshold as a multiple of the modelled aperiodic component.

While oscillation detection methods have advanced considerably, two main challenges remain. First, as noted above, oscillations must manifest as narrow-band peaks in the power spectrum (Donoghue et al., 2022; Gross, 2014; Lopes da Silva, 2013). Within the family of BOSC algorithms, all frequency bins exceeding the power threshold are considered potential oscillations. However, it is only the frequency peak in the power spectrum that

defines the underlying oscillation. This is of particular importance when multiple frequencies coexist (e.g., 10 and 20 Hz), as only their respective peaks indicate genuine oscillations, whereas intermediate frequencies (e.g., 15 Hz), even if they exceed the power threshold, do not reflect true oscillatory activity. The second challenge is the identification of oscillatory episodes across different brain regions. Existing methods are typically limited to single-channel electrophysiological signals, yet a comprehensive characterization of brain oscillations requires incorporating multi-channel information, as provided by magneto-/electroencephalography (M/EEG) recordings. Furthermore, the identification of oscillations at the sensor level does not necessarily imply the presence of an underlying neural generator, since rhythmic fluctuations in the M/EEG signal can arise from multiple factors (Cohen, 2017; Jackson & Bolger, 2014; Van Bree et al., 2024). In contrast, detecting oscillations directly at the source level would enable the identification of the underlying oscillatory generators, thereby enhancing interpretability.

To address these challenges, we have developed an algorithm within the BOSC framework to detect episodes of brain oscillatory activity at the source level in electrophysiological data (M/EEG). The method, called pBOSC for *peak*-BOSC, incorporates a number of improvements. First, to ensure the detection of genuine oscillatory activity, only *peaks* in the power spectrum are selected. Second, we only take into consideration oscillatory activity in voxels presenting a *peak* or local maximum in oscillatory power, thus mitigating undesired source leakage effects. In this study, we validated pBOSC by applying it to a series of simulated signals with varying parameters, such as oscillatory frequency, number of cycles, generator depth, and signal-to-noise ratio (SNR). Additionally, pBOSC was applied to real resting-state MEG data to assess whether the natural frequencies (i.e., the most characteristic oscillatory frequencies at each voxel), estimated using this method were consistent with those reported in previous studies (Capilla et al., 2022).

2. Methods

Here, we have developed pBOSC, a method designed to detect oscillatory episodes in electrophysiological brain signals. As in previous BOSC variants, oscillatory episodes were defined as segments of the signal that exceed both a power threshold and a duration threshold. The power threshold was set at the 95th percentile of the power of the aperiodic component. Furthermore, only peaks identified in both the power spectrum and the brain volume were retained to ensure the selection of genuine oscillatory activity. The duration threshold required a minimum of three complete cycles to confirm rhythmicity.

To validate pBOSC, we applied it to simulated as well as real resting-state MEG data. The following sections describe the generation of the simulated data and the acquisition procedures for real MEG recordings. We then provide a detailed description of the pBOSC algorithm, followed by an explanation of how both datasets were analyzed to evaluate the performance and validity of the method. All code was written in MATLAB (2024b; The MathWorks Inc, 2024), with additional functions from FieldTrip (version 20230118;Oostenveld et al., 2011), fBOSC (Seymour et al., 2022), and FOOOF (Donoghue et al., 2020). The full code required to reproduce the method, analyses, and figures in this work is openly available at https://github.com/necog- UAM/.

2.1. Generation of simulated data

To evaluate the performance of pBOSC, we simulated brain oscillatory activity embedded in realistic background noise (Figure 1). Data from a randomly selected participant (see section 2.3) were used as a template to generate both a simulated brain volume and the MEG sensor coordinates. A pure sinusoidal oscillation was first generated at a specific voxel and time window and then projected onto the sensor space. To mimic the coexistence of oscillatory and aperiodic components in real electrophysiological recordings, pink noise—a

hallmark of aperiodic activity—was generated at five semi-random brain locations using the *cnoise* function implemented in fBOSC (Seymour et al., 2022). Candidate voxels for aperiodic sources were constrained to lie at least 1.5 cm away from oscillatory sources, thus minimizing contamination and ensuring the spatial specificity of oscillation localization. Aperiodic activity was subsequently projected onto the sensors. Additionally, white noise with an amplitude equivalent to the median of the aperiodic activity was added to account for stochastic noise inherent to MEG recordings. Finally, the oscillatory, aperiodic and white noise components were linearly combined to obtain the simulated signal.

We simulated multiple datasets by systematically varying different parameters that could potentially influence the detection performance of pBOSC: oscillatory frequency (5, 10, and 20 Hz), number of cycles (3, 10, and 20 consecutive cycles), generator depth (65, 75, and 85 mm from the MEG sensors), and SNR (0.5, 1.0, and 1.5). SNR was computed as the ratio between the root mean square (RMS) of the sinusoidal oscillation and the RMS of the pink noise in the sensor exhibiting the strongest projection of oscillatory activity. In addition, to ensure that the spatial configuration of the aperiodic sources did not affect pBOSC performance, the simulation procedure was repeated five times for each parameter combination, using a new set of semi-randomly selected pink noise voxels in each repetition. Therefore, for each of the four parameters (e.g., oscillatory frequency), we generated three different signals (e.g., 5, 10, and 20 Hz), and repeated the process five times, resulting in a total of 405 simulated signals ($3^4 \times 5$).

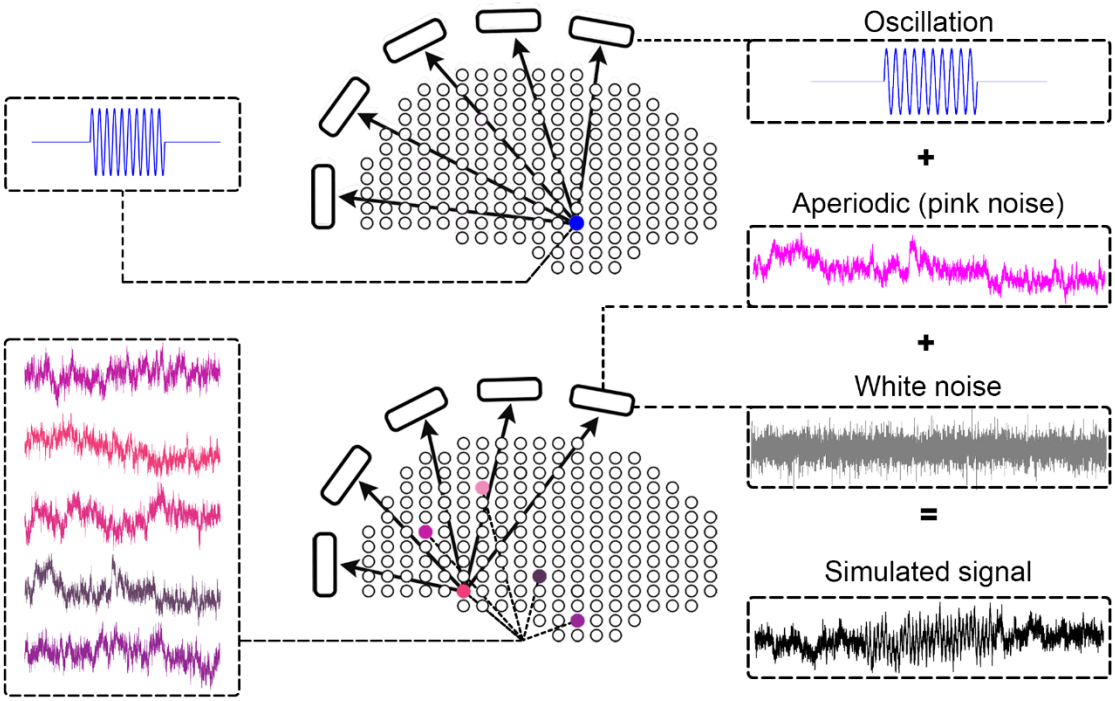

Figure 1. Simulation of brain signals in MEG sensors. A sinusoidal oscillation was generated at a specific voxel in the brain and projected onto the sensors (blue). Pink noise was generated at five semi-randomly selected voxels and subsequently projected onto the sensors (pink). Oscillatory activity, pink noise, and white noise (gray) were linearly combined to create the simulated brain signal in sensor space (black).

2.2. Acquisition and pre-processing of resting-state MEG data

Anonymized resting-state MEG recordings and T1-weighted Magnetic Resonances Images (MRIs) were downloaded from the open-access OMEGA database (Niso et al., 2016). Data acquisition took place at the Montreal Neurological Institute (MNI, McGill University), with approval from the institutional ethics committees and in accordance with the declaration of Helsinki. MEG recordings were acquired using a whole-head CTF MEG system equipped with 275 axial gradiometers and 26 reference sensors, within a magnetically shielded room. The MEG signal was digitized at a sampling rate of 2400 Hz and recorded with a 600 Hz low-pass anti-aliasing filter. Individual head shapes and three anatomical landmarks (nasion, left- and right- pre-auricular points) were also digitized to facilitate MEG-MRI co-registration.

We analyzed data from 128 healthy participants (68 males, 118 right-handed, mean age 30.5 ± 12.4 [M ± SD], range 19-73 years) who were sitting upright and instructed to maintain a relaxed wakeful state with their eyes open, fixating on a cross for five minutes. In this study, we used data that had been preprocessed in a previous work (Capilla et al., 2022). In brief, MEG signals were denoised and filtered with a 0.05 Hz high-pass filter. Power line noise and its harmonics were reduced using spectrum interpolation. Finally, artifactual components related to cardiac, ocular, and muscular activity were removed using Independent Component Analysis (ICA), and contaminated data segments were excluded from further analysis.

2.3. Detection of oscillatory episodes using pBOSC

The pBOSC algorithm comprises the following eight steps: (1) reconstruction of source-level activity, (2) estimation of the aperiodic component, (3) correction of the center of the head bias, (4) time-frequency decomposition, (5) identification of the power threshold, (6) detection of peaks in the power spectra, (7) detection of peaks in the brain volumes, and (8) selection of oscillatory episodes exceeding the duration threshold. These analysis steps are illustrated in Figure 2 and explained in more detail in the next paragraphs.

(1) Reconstruction of source-level activity. Since pBOSC has been designed to detect oscillatory activity directly in source space, the first step involves reconstructing the source-level time series from the MEG sensor data. The co-registration of each participant's T1-weighted MRI and the MEG head coordinate space was obtained from Capilla et al. (2022) (https://github.com/necog-UAM/OMEGA-NaturalFrequencies/tree/main/coregistration). For the simulated data, one randomly selected participant served as a template for defining the brain volume and MEG sensor locations used in every simulation. From this point onward, the analysis pipeline was identical for both the simulated and real data. A realistic single-shell

volume conduction model (Nolte, 2003) was employed to compute the lead fields on a 1 cm resolution grid. Source-level time series were then reconstructed using linearly constrained minimum variance beamforming (LCMV; Van Veen et al., 1997). The covariance of the artifact-free data served to calculate the spatial filter weights, with the regularization parameter lambda adjusted to 10%. Lastly, beamforming weights were applied to reconstruct source-space time series from the sensor-level data (Figure 2a).

(2) Estimation of the aperiodic component. Similarly to fBOSC and PAPTO, we estimated the aperiodic component from the source-reconstructed time series using the FOOOF algorithm (Donoghue et al., 2020). The estimation of the aperiodic activity served two purposes. First, it was employed to correct the center of the head bias, which is inherent in beamforming source reconstruction (step 3). Second, it provided the basis for determining the power threshold above which oscillations can be identified (step 5). Instead of computing a single aperiodic estimate for the entire signal, we applied FOOOF to shorter time windows, each lasting 20 seconds, to capture potential dynamic variations. The estimate of the aperiodic component extracted from each time window was transformed back into the time domain (Figure 2b). In this way, we obtained a signal containing only the aperiodic time series derived from FOOOF, subjected from that point onward to the same analysis procedures as the original signal.

(3) Correction of the center of the head bias. Beamformer source estimates are biased toward the center of the head, which exhibits stronger activity compared to cortical areas (Shapira Lots et al., 2016). This is typically corrected by normalizing the source-reconstructed activity with an estimate of noise. In Capilla et al. (2022), noise was estimated from the RMS of source-level data for each voxel. However, regions with high-amplitude oscillatory activity also tend to have high RMS values. For this reason, in this study, we estimated noise using the RMS of the signal containing only the aperiodic component, which,

by definition, do not contain structured oscillatory activity. Thus, the center of the head bias was corrected in both the original and the aperiodic time series by normalizing them with the RMS of the aperiodic time series.

(4) Time-frequency decomposition. After downsampling the signal to 128 Hz to reduce computational load, a time-frequency decomposition was performed on both sets of data (original and signal containing only the aperiodic component) using the same parameters (Figure 2c). Power values were extracted for 32 logarithmically spaced frequency bins, ranging from 1.8 to 40.5 Hz, using the Short-Time Fourier Transform (STFT) with a Hanning-tapered sliding window. The window length was adaptive, dynamically adjusted to cover 5 cycles of the frequency being analyzed. Previous BOSC variants have typically employed wavelet decomposition for time-frequency analysis. However, wavelets and STFT with a Hanning sliding window set to a fixed number of cycles per frequency produce largely equivalent results (Bruns, 2004).

(5) Identification of the power threshold. For each voxel and frequency, the power threshold was set to the 95th percentile of the power derived from the signal containing only the aperiodic component across all time points. Thus, only time-frequency points exceeding this power threshold were considered potential candidates for oscillations in subsequent analysis.

(6) Detection of peaks in the power spectra. Since oscillations should exhibit a spectral peak (Donoghue et al., 2022; Gross, 2014; Lopes da Silva, 2013), local maxima were identified in the power spectra for every voxel and time point. Data points that fulfilled this criterion were tagged as candidates for oscillations (Figure 2d).

(7) Detection of peaks in the brain volumes. Additionally, due to the ill-posed nature of the inverse source reconstruction problem, the so-called spatial or source leakage poses a

significant challenge (O'Neill et al., 2015). In brief, while brain activity may originate from a single voxel, it can spread across a larger region of adjacent voxels, none of which are true generators. To address this issue, we computed local maxima of spectral power across the 3D brain volumes and considered only the previously identified spectral peaks that also corresponded to a spatial peak within the brain (Figure 2e).

(8) Selection of oscillatory episodes exceeding the duration threshold. Similarly to previous algorithms, we established a duration threshold to discard spurious and non-oscillatory transient brain events (Caplan et al., 2001; Kosciessa et al., 2020; Seymour et al., 2022). Thus, only episodes lasting at least three consecutive cycles were considered oscillatory episodes. To prevent false negatives due to brief power drops, sequential oscillatory bursts with the same frequency and appearing in the same voxel area (within a 1.5 cm radius) were merged if the temporal gap between them was less than half a cycle (Figure 2f).

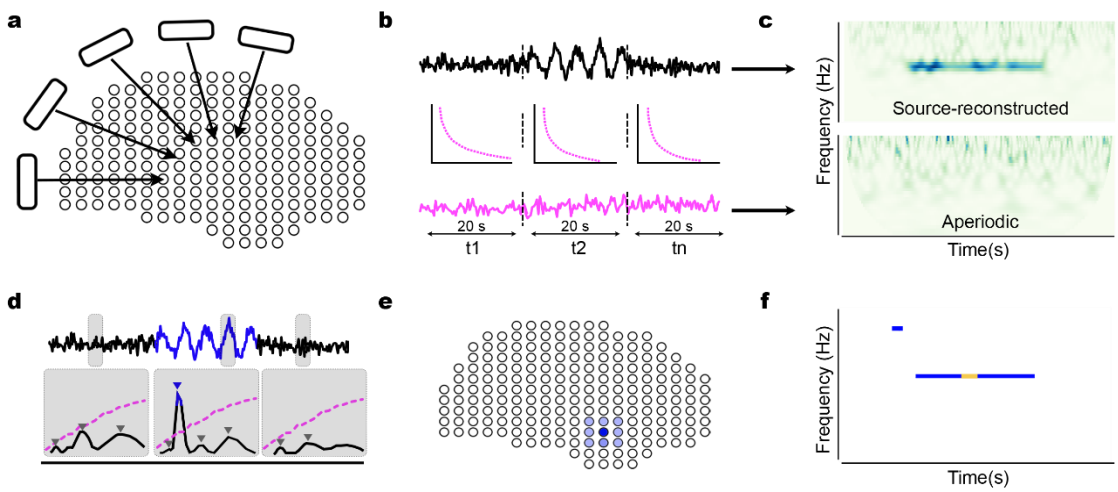

Figure 2. Detection of oscillatory episodes using pBOSC. a. The pre-processed MEG signal is reconstructed in source space using beamforming. **b.** The aperiodic component is extracted from the signal using FOOOF in 20-seconds time windows and transformed back to time domain. **c.** Time-frequency decompositions of the source-reconstructed signal and the signal containing only the aperiodic component are computed using STFT. **d.** Only time-frequency points that exceed the power threshold (95th percentile of the aperiodic component

signal, dashed pink line) and display a peak in the power spectrum (triangle markers) are tagged (blue) as candidates for oscillations. Three illustrative spectra extracted are shown (gray boxes). **e.** To mitigate spatial leakage effects, only local maxima in the brain volume are considered oscillation generators. **f.** Adjacent time-frequency points are connected to define oscillatory episodes, provided that at least three consecutive cycles are detected. A transiently discontinuous episode is highlighted (yellow) and merged to form a continuous oscillatory episode. A false alarm can be observed (left corner).

2.4. Analysis of simulated data

We applied pBOSC to the simulated data to evaluate its performance under controlled conditions. For each simulation, hits and false alarms were quantified by averaging the outcomes across the five repetitions per parameter set. A hit, or correct detection, was defined as an episode detected at the same frequency and time points as simulated, and within a 1.5 cm radius of the true source location, thus accounting for slight inaccuracies in source reconstruction. False alarms were defined as the total number of data points identified as episodes in the absence of simulated oscillations. To further examine the impact of the different parameters on pBOSC performance, we conducted one-way analyses of variance (ANOVAs) to compare the number of hits across all parameter settings (oscillatory frequency, number of cycles, generator depth, and SNR). Additionally, we verified that the semi-random location of the aperiodic generators did not affect the detection of oscillatory episodes.

2.5. Analysis of real MEG data

In addition to the simulations, we also applied pBOSC to real resting-state MEG data (Niso et al., 2016). This resulted in a matrix of detected oscillatory episodes, organized as time-points by frequencies, for each voxel within the cerebral cortex (1925 voxels) and for each participant (N = 128).

To compute the brain's natural frequencies, which represent its most characteristic oscillatory patterns, the total number of detected oscillatory cycles per participant, voxel, and frequency was summed across time. The resulting matrix was then z-score normalized across voxels to identify the frequency with the highest number of oscillatory cycles in each voxel This normalization procedure minimizes the dominance of the alpha rhythm (Capilla et al., 2022).

Natural frequencies at the group level were estimated following the bootstrapping procedure described by Capilla et al. (2022) to enable direct comparison with their results. In brief, participants were sampled with replacement 500 times. In each iteration, a histogram of the natural frequencies for each voxel was computed. Subsequently, we fitted a Gaussian function to all candidate peak frequencies and selected the peak with the highest goodness-of-fit. Each voxel's natural frequency was then defined as the median value across bootstrap iterations. This method is preferred over the group mean, as some participants may have very extreme natural frequencies in the same voxel due to several reasons, including sharp transitions between nearby anatomical regions or limitations in the accuracy of source localization. Finally, we validated our results by comparing the obtained map of natural frequencies with the one reported by Capilla et al. (2022). A Pearson correlation analysis was performed to assess the voxel-by-voxel similarity between the natural frequencies derived from both approaches. Additionally, for comparative purposes, we also computed the natural frequencies for 40 regions defined by the Automated Anatomical Labeling (AAL) atlas (Tzourio-Mazoyer et al., 2002).

3. Results

To assess the effectiveness of pBOSC in detecting oscillatory activity, we first applied the method to a series of simulations, analyzing the impact of different parameters on

detection performance. Subsequently, pBOSC was applied to real resting state MEG data to identify the brain's natural frequencies at the single-voxel level, and these results were then compared with those obtained by Capilla et al. (2022).

3.1. Detection performance of pBOSC on simulated data

We applied pBOSC to a total of 405 simulations, each defined by a unique set of oscillatory activity and noise features. Oscillatory activity was simulated by a pure sine wave with different oscillatory frequencies (5, 10, and 20 Hz), number of cycles (3, 10, and 20 consecutive cycles), generator depth (65, 75, and 85 mm from the MEG sensors), and SNR (0.5, 1, and 1.5). The aperiodic component was simulated by adding the contribution of five generators of pink noise with semi-random locations to the signal (5 repetitions). After applying pBOSC, we computed hits and false alarms for each set of parameters simulated.

The results of the one-way ANOVA on the number of hits across repetitions showed that repetitions did not affect detection performance ($F_{(4,400)} = .763$, $p = .549$), thus ensuring that the semi-random location of the pink noise generators did not influence the results. Additionally, distance from the signal source to the sensors (depth) was also not statistically significant ($F_{(2,78)} = 1.433$, $p = .244$). This was expected as SNR was adjusted independently of voxel depth. On the contrary, frequency ($F_{(2,78)} = 6.082$, $p = .003$; $\eta_p^2 = .134$), number of cycles ($F_{(2,78)} = 4.971$, $p = .009$; $\eta_p^2 = .113$, and SNR ($F_{(2,78)} = 9.586$, $p < .001$; $\eta_p^2 = .197$) significantly altered the number of hits detected with pBOSC. Specifically, lower frequencies (5 Hz), longer duration (20 cycles), and higher SNR (1.5) resulted in significantly greater number of hits compared to their counterparts (Figure 3).

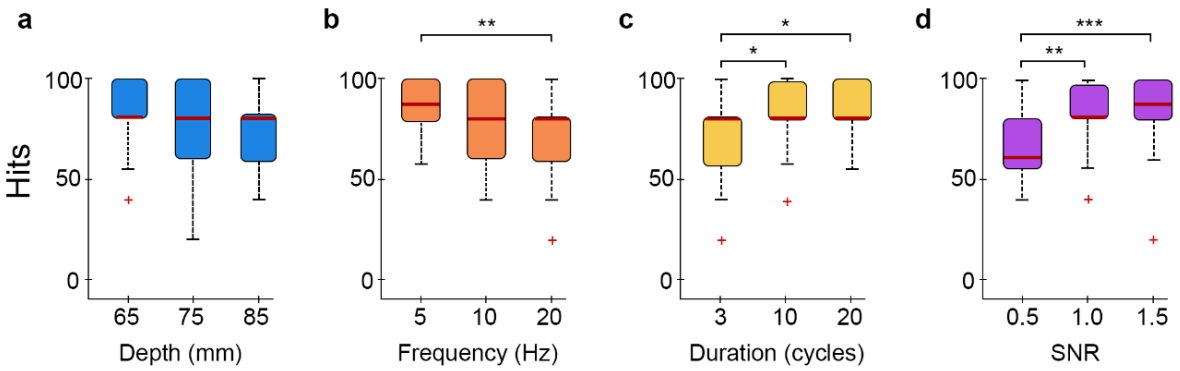

Figure 3. Influence of simulation parameters on pBOSC performance. Percent of hits across different parameter sets. Red bars inside the boxes represent the median value. Significant post-hoc differences are indicated with asterisks (* p < .05, ** p <.01, *** p < .001). **a.** Hits in simulations with varying depth from sensors. **b.** Hits in simulations with different frequency values. **c.** Hits in simulations with varying duration (number of cycles). **d.** Hits in simulations with different SNR values.

Since neither depth not the location of the pink noise generators showed statistically significant effects, we averaged hits and false alarms across these conditions to compute an overall performance of pBOSC. Figure 4 shows the resulting hits and false alarms for each scenario. Correct detection of oscillatory episodes was on average 66% at the lowest SNR levels, increasing to 82% at medium SNR and up to 86% at higher SNR levels. Importantly, false alarms remained stable across different SNR levels, staying below 0.1% in all scenarios.

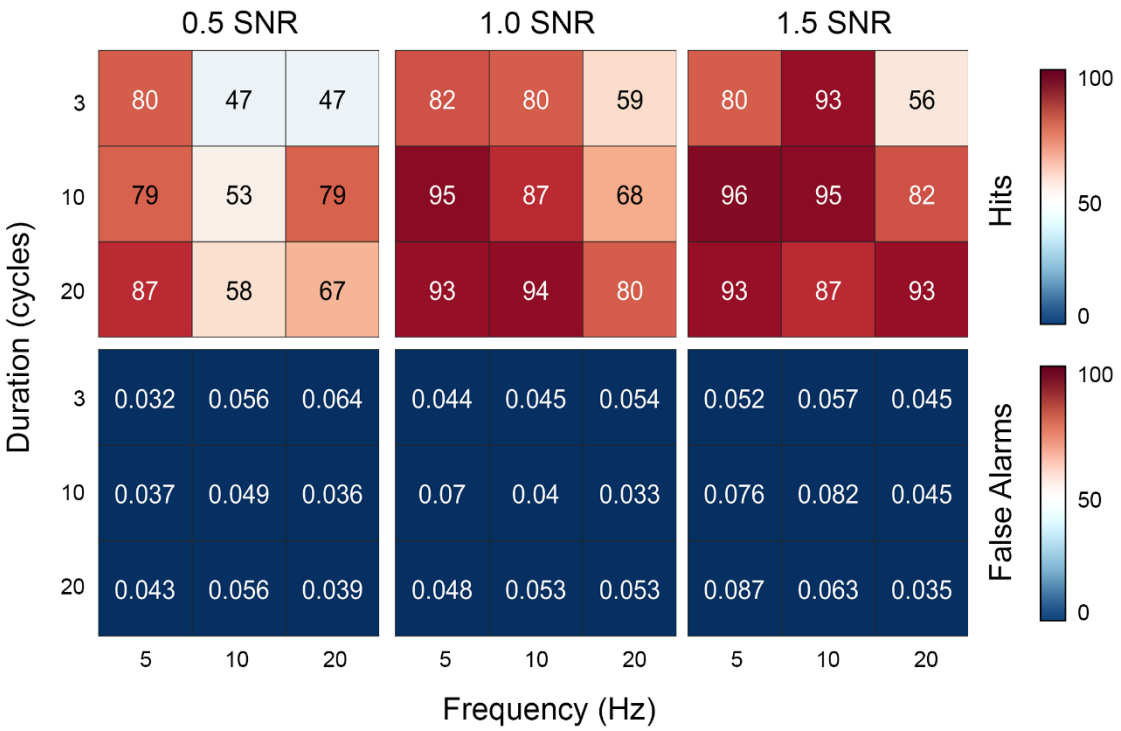

Figure 4. Detection performance of pBOSC in the simulated data. Hits (top panels) and false alarms (bottom panels) across different scenarios, each defines by a combination of oscillatory frequency, number of cycles and SNR levels. Parameter combinations resulting in the highest hit performance can be seen in warmer colors, while lower false alarm rates are shown in cooler colors.

Oscillatory episodes were accurately localized within a 1.5 cm radius of their simulated sources in 75% of all simulations. Among the remaining 25% of oscillatory episodes that were detected but mislocalized, 50% were localized within a 2.5 cm radius of their generators, while the other half decreased progressively with increasing distance. Only 15% of the mislocalized episodes (0.038% of all simulations) were found beyond 6.5 cm from their original location. Moreover, half of the mislocalized episodes occurred in the lowest SNR scenario. In an ideal scenario (slowest frequency, longest duration and highest SNR), the localization error is drastically reduced, with nearly all oscillatory episodes accurately localized within their sources.

3.2. Characterization of the brain's natural frequencies using pBOSC on real MEG data

Finally, we applied pBOSC to a real set of resting-state MEG data. The supplementary material contains a video clip illustrating the detected oscillatory episodes for a representative participant (Supplementary Video 1). The same dataset had previously been used by Capilla et al. (2022) to identify the brain's natural frequencies through k-means clustering of power spectra. Here, we aimed to test whether pBOSC could achieve similar results by detecting the most characteristic oscillatory frequency for each voxel. The comparison between the natural frequency map obtained using pBOSC and the original map is shown in Figure 5. Overall, the two maps exhibit a high degree of similarity, as indicated by a Pearson correlation coefficient of 0.61 ($p<.001$).

Both the voxel wise brain map and the distribution of natural frequencies across AAL regions exhibited a similar pattern between the two approaches. Delta frequency values (δ; 2-4 Hz) were characteristic of the orbitofrontal cortex and certain temporal regions. Theta (θ; 4 -8 Hz) represented the natural frequency of the medial frontal cortex. Alpha-band oscillations (α; 8-12 Hz) were distributed over parieto-occipital regions, although some areas of the parietal cortex showed a natural frequency within the low-beta instead of the alpha band using pBOSC. Finally, beta-band oscillations (β; 13-30 Hz) were characteristic of the somatomotor and lateral prefrontal cortices. The largest discrepancies were found in frontal and temporal areas, where transitions occurred between low delta frequencies in the temporal lobe and high beta in frontal regions.

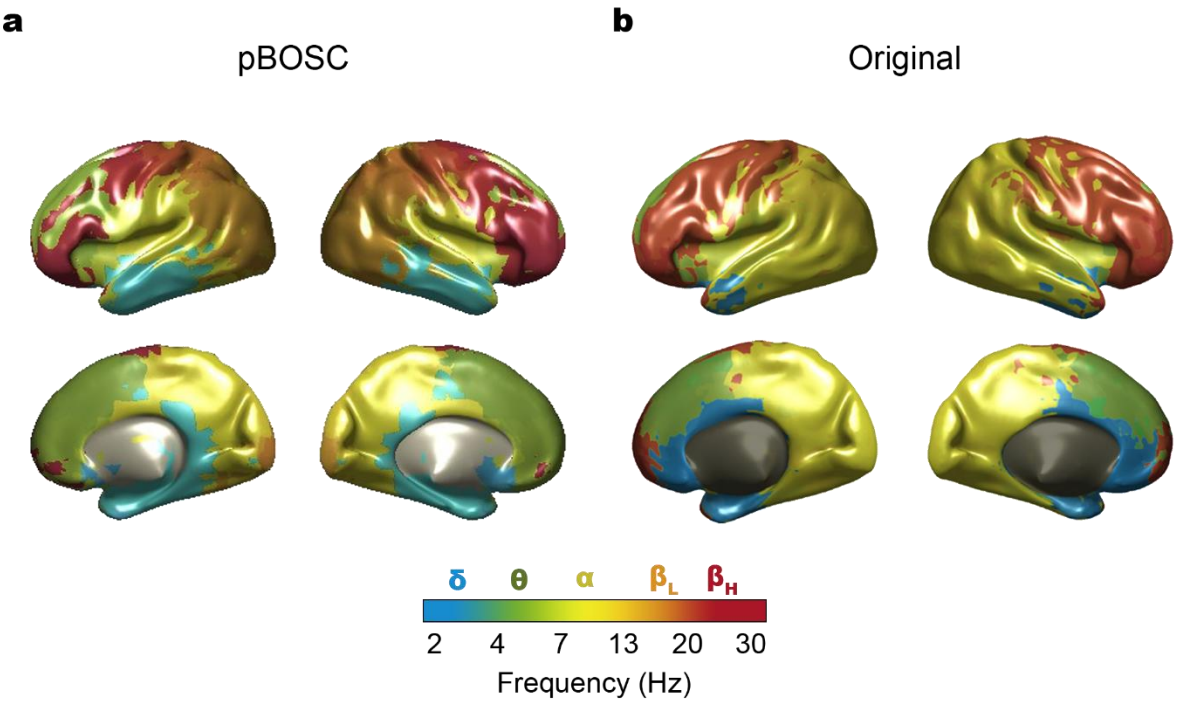

c

	pBOSC	Original
Precentral gyrus	27.1	22.6
Superior frontal gyrus (dorsolat)	6.9	23.0
Superior frontal gyrus (orb)	6.9	23.3
Middle frontal gyrus	28.7	23.5
Middle frontal gyrus (orb)	33.4	25.3
Inferior frontal gyrus (oper)	27.5	22.9
Inferior frontal gyrus (tri)	28.6	23.1
Inferior frontal gyrus (orb)	28.9	23.6
Rolandic operculum	9.8	8.4
Supplementary motor area	6.7	5.5
Olfactory cortex	2.5	2.1
Superior frontal gyrus (med)	6.8	5.6
Superior frontal gyrus (med orb)	6.9	23.4
Rectus gyrus	6.8	2.1
Insula	6.9	22.6
Anterior cingulate gyrus	6.9	5.4
Middle cingulate gyrus	10.6	10.2
Posterior cingulate gyrus	3.5	10.0
Hippocampus	3.5	2.4
Parahippocampal gyrus	3.5	2.3

	pBOSC	Original
Calcarine cortex	10.4	10.4
Cuneus	10.7	10.5
Lingual gyrus	10.6	10.3
Superior occipital gyrus	11.9	10.3
Middle occipital gyrus	14.9	11.9
Inferior occipital gyrus	14.6	10.4
Fusiform gyrus	3.6	2.3
Postcentral gyrus	21.7	21.4
Superior parietal gyrus	11.8	11.5
Inferior parietal gyrus	18.2	12
Supramarginal gyrus	9.9	11.9
Angular gyrus	15.1	12
Precuneus	10.6	10.4
Paracentral lobule	11.7	11.8
Heschl gyrus	10.1	10.1
Superior temporal gyrus	9.9	9.8
Temporal pole (sup)	8.1	23.1
Middle temporal gyrus	12	9.9
Temporal pole (middle)	3.5	23.2
Inferior temporal gyrus	3.6	10.1

Figure 5. Brain map of natural frequencies derived using pBOSC. a. Natural frequencies extracted from the oscillatory episodes detected with pBOSC. **b.** Natural frequencies obtained by Capilla et al. (2022) [Reproduced with permission]. **c.** Comparison of the natural frequencies across different AAL regions obtained with both methods. The color scale represents frequency (ranging from blue: delta band, to red: high-beta). White to black squares indicate the absolute difference in natural frequency between the two methods for each region.

4. Discussion

In this study, we developed and validated a novel method for detecting oscillatory episodes in electrophysiological data. This method, which we termed pBOSC, builds upon the BOSC family of algorithms (Caplan et al., 2001; Kosciessa et al., 2020; Seymour et al., 2022; Whitten et al., 2011) and addresses two major limitations in current oscillation detection approaches. First, because true oscillations should manifest as spectral peaks rising above the aperiodic background (Donoghue et al., 2022; Gross, 2014; Lopes da Silva, 2013), our approach identifies local maxima in the frequency spectrum to distinguish broad-band high-power events from frequency-specific peaks. Secondly, most existing methods are restricted to single-channel signals in sensor space, whereas a comprehensive analysis of brain oscillations requires examining the neural sources generating that activity. With pBOSC, we have taken a step forward in the detection of oscillatory episodes by addressing both limitations. We first validated pBOSC through a series of simulations with different signal properties, and then evaluated its performance on real resting-state MEG data.

4.1. pBOSC performance on simulated data

We evaluated the detection performance of pBOSC through a series of simulations defined by unique parameter combinations, included the location of the aperiodic component within the brain, the position of the oscillatory generators, their distance to the nearest sensor, oscillation frequency, number of cycles and SNR. We analyzed the algorithm's performance across these different simulated scenarios.

The aperiodic component was semi-randomly generated at five locations within the brain, and this procedure was repeated five times for each unique parameter combination. No significant differences were observed between repetitions, thereby confirming that the location of the aperiodic generators did not affect pBOSC's detection accuracy. Similarly, the location of the oscillatory sources did not influence detection performance either. Given the

independent manipulation of the oscillation SNR regardless of the generator depth, we expected the location of the oscillator to have minimal or no effect.

We also evaluated the frequency and the number of cycles of the simulated oscillations. Significant differences emerged between the three frequencies analyzed, with the slowest frequency (5 Hz) being detected more often than the fastest frequency (20 Hz). Similarly, significant differences were found between the number of cycles, where the conditions with the greatest number of cycles (10 and 20 cycles) yielded higher hit rates compared to the condition with the fewest (3 cycles). Both results can be explained by the total length of the oscillation, which increases with either a lower frequency or a higher number of complete cycles. Nonetheless, brain electrophysiological data contain oscillations from approximately 0.05 Hz up to 500 Hz (Buzsáki & Draguhn, 2004) that can last from short-lived transient bursts (Jones, 2016; Van Ede et al., 2018; Vidaurre et al., 2016) to several sustained cycles as in the case of posterior alpha oscillations. This implies that faster and/or shorter oscillatory activity may be challenging to detect with pBOSC. Moreover, pBOSC, along with other current oscillation detection methods, establishes a minimum requirement of three complete cycles for a given frequency to be considered an oscillatory episode. This threshold reduces the false categorization of random fluctuations in power as an oscillatory episode but comes at the cost of overlooking genuine transient oscillatory bursts that last less than three cycles. Thus, identifying oscillations occurring at shorter time scales remains a challenge. One possible approach for detecting transient brain states of brief duration is the use of Hidden Markov Models (HMM) (Quinn et al., 2019), although their direct relation to oscillatory neural activity is not yet fully understood.

Lastly, we assessed pBOSC performane across three different SNR scenarios, in which noise was higher (0.5), equal (1.0) or lower (1.5) relative to the signal amplitude. As expected, the algorithm yielded the highest detection accuracy (86%) when the signal

amplitude was 50% greater than the noise. Even when signal and noise amplitudes were equal, accuracy remained high (82%), but declined (66%) in the most challenging condition, where noise exceeded the signal by 50%. It is worth noting that, in real MEG data, SNR is not constant but fluctuates across time, source location, and participants, resulting in mixed SNR conditions throughout the recording.

Overall, simulation results demonstrate that pBOSC is a robust algorithm for detecting oscillatory episodes in multi-channel electrophysiological data, consistently achieving high detection rates and very low false alarm rates. Detection performance is modulated by oscillation length and SNR, with longer-lasting oscillations and higher SNR yielding the most accurate results.

4.2. pBOSC performance in resting-state MEG data

After validating the method through simulations, pBOSC was subsequently applied to real MEG data. The same participant dataset had previously been analyzed by Capilla et al. (2022) to extract a map of natural frequencies, which served as a benchmark for evaluating the results obtained with pBOSC. Once oscillatory episodes were identified, natural frequencies were computed as the frequency with the highest number of oscillatory episodes at each voxel. Group-level values were then calculated using the same bootstrapping procedure as Capilla et al. (2022) to ensure comparability.

Despite relying on different approaches to estimate natural frequencies (k-means clustering of power spectra versus oscillatory episode detection), both methods yielded consistent results, as evidenced by a strong voxel wise correlation ($r = 0.61$). Both approaches captured key oscillatory patterns. Delta frequencies were characteristic of the orbitofrontal and medial temporal regions, although pBOSC showed a broader extension over the temporal lobe compared to previous findings. This increased sensitivity to low-frequency oscillations

may stem from explicitly removing the aperiodic component, which typically dominates the lower-frequency spectrum. Frequencies within the theta range consistently characterized the mid-frontal cortex. Alpha oscillations were the distinctive frequency of the posterior lobes, while parietal and lateral occipital regions were characterized by frequencies in the low-beta band. Finally, higher frequencies were predominant in motor and prefrontal regions.

The frequency distribution identified with pBOSC is also in agreement with previously reported resting-state relative power maps derived from MEG (Keitel & Gross, 2016; Mellem et al., 2017; Niso et al., 2016) and iEEG data (Afnan et al., 2023; Kalamangalam et al., 2020).

4.3. Comparison with other oscillation detection methods

A direct comparison of pBOSC with existing oscillation detection methods is limited due to the distinct scope of pBOSC. Methods such as the BOSC family (Caplan et al., 2001; Kosciessa et al., 2020; Seymour et al., 2022; Whitten et al., 2011) and PAPTO (Brady & Bardouille, 2022) are designed to identify oscillatory episodes in single-channel data. In contrast, pBOSC is specifically designed to detect the underlying sources of oscillations measured at the multi-channel level. While existing methods can be applied to source-reconstructed data, the nature of the oscillatory episodes they detect differs from those identified by pBOSC. Oscillatory episodes detected by existing methods in source-reconstructed data would indicate the presence of an oscillation at a given location, whereas pBOSC categorizes activity as an oscillatory episode only if the oscillation represents a local maximum at that location. Ideally, this implies that locations where oscillatory episodes are identified correspond to genuine oscillators.

In practice, however, due to the combined influence of factors such as SNR, dipole orientation, and the inherent imprecision of source-reconstruction algorithms, the identified

location cannot be guaranteed as the true oscillatory generator (Brunner et al., 2016; Jonmohamadi et al., 2014; Van Den Broek et al., 1998; Van Veen et al., 1997; Westner et al., 2023). In fact, as demonstrated in our simulations, oscillatory episodes identified more than 1.5 cm away from the actual generator were treated as misses, even though their frequency and timing were correctly recovered. This occurred in 25% of the total simulations. While pBOSC is designed to detect oscillatory episodes originating from their true underlying sources, caution is warranted when inferring that any particular episode location corresponds to a genuine oscillator.

4.4. Applicability and remaining challenges

Several advantages arise from detecting oscillatory episodes directly, rather than interpreting relative power changes, as it is often done in M/EEG research by subtracting a baseline window presumed to containing no relevant activity (Gross, 2014; Gyurkovics et al., 2022).

First, pBOSC allows for the effective analysis of electrophysiological signals in situations where baseline windows are not available, such as resting-state recordings or experimental tasks with short intertrial intervals, while still accounting for the pervasive aperiodic activity. To extract the aperiodic component, 20 second segments were used as a trade-off between computational efficiency and sufficient sensitivity to track dynamic fluctuations in aperiodic activity over time (Gao et al., 2017). However, this time interval could be adapted to match the duration of individual trials, making the method suitable for time-segmented recordings.

Second, analyzing relative power changes in the power spectrum may lead to misleading interpretations of oscillatory brain activity, as these changes can reflect variations in the aperiodic component rather than genuine oscillatory dynamics (Donoghue et al., 2022).

By focusing only on activity that exhibits a local maximum above the aperiodic background, pBOSC ensures that the analysis targets true oscillatory phenomena, thereby avoiding misinterpretations driven by non-oscillatory power fluctuations.

Third, detecting oscillatory episodes directly in source space might substantially simplify connectivity analyses, which often explore relationships across various signal features (e.g., amplitude, phase or phase-amplitude coupling) across multiple frequencies and brain regions. Focusing on segments where oscillatory episodes are identified at specific locations would help narrow down the vast number of potential hypotheses, thereby reducing the computational load and increasing the interpretability of connectivity results.

While pBOSC offers potential benefits, it also has some limitations. First, it is tuned to detect episodes with a minimum duration of three cycles. This conservative threshold serves to filter out noisy transients but may also exclude genuine short-lived oscillatory bursts (Jones, 2016; Van Ede et al., 2018; Vidaurre et al., 2016). However, the method can be adapted to identify shorter episodes if needed at the cost of increasing the number of false alarms.

A second problem arises when interpreting the location of identified episodes as their true generators. Although most of our simulations successfully recovered the original sources of the oscillations, this limitation is inherent to the ill-posed nature of source-reconstruction algorithms (Brunner et al., 2016; Jonmohamadi et al., 2014; Van Den Broek et al., 1998; Van Veen et al., 1997). Accurate identification of oscillatory episodes depends not only on pBOSC's detection performance but also con the precision of beamformer reconstruction. Consequently, an oscillatory episode that is correctly detected by pBOSC may still be considered a miss if the beamformer's reconstructed location deviates from the true source.

This limitation is likely to be more pronounced when applying pBOSC to EEG rather than MEG signals, as volume conduction effects reduce the precision of source reconstruction.

5. Conclusion

In this work, we introduce pBOSC, an algorithm designed to detect oscillatory episodes in electrophysiological data. We validated the method using both simulated and real datasets. This algorithm extends the BOSC family of methods by supporting multi-channel data and ensuring the presence of oscillatory activity above the aperiodic background. pBOSC offers a complementary approach for studying oscillatory dynamics at the source level, enabling the identification of non-averaged oscillatory events over time and opening new avenues for measuring brain connectivity.

Code and availability

The full code required to reproduce the method, analyses, and figures in this work is openly available at https://github.com/necog- UAM/.

Author Contributions

Enrique Stern: Conceptualization, Data curation, Formal analysis, Methodology, Software, Visualization, Writing– original draft preparation; **Guiomar Niso**: Conceptualization, Writing – Review & editing; **Almudena Capilla**: Conceptualization, Data curation, Funding acquisition, Methodology, Writing – original draft preparation.

Declaration of Competing Interest

The authors declare no competing interests.

Acknowledgements

We are thankful to the contributors of Open MEG Archive (OMEGA) for providing the publicly available dataset used in this work.

This work was supported by Ministerio de Ciencia e Innovación / Agencia Estatal de Investigación, Spain / FEDER/FSE+, UE (MCIN/AEI/ 10.13039/501100011033 /FEDER/FSE+, UE; grants PRE2022-101613 to ES, RYC2021-033763-I and PID2023-150034OA-I00 to GN, and PID2021-125841NB-I00 to AC).

References

Afnan, J., Von Ellenrieder, N., Lina, J.-M., Pellegrino, G., Arcara, G., Cai, Z., Hedrich, T., Abdallah, C., Khajehpour, H., Frauscher, B., Gotman, J., & Grova, C. (2023). Validating MEG source imaging of resting state oscillatory patterns with an intracranial EEG atlas. *NeuroImage*, *274*, 120158. https://doi.org/10.1016/j.neuroimage.2023.120158

Bonnefond, M., Kastner, S., & Jensen, O. (2017). Communication between Brain Areas Based on Nested Oscillations. *Eneuro*, *4*(2), ENEURO.0153-16.2017. https://doi.org/10.1523/ENEURO.0153-16.2017

Brady, B., & Bardouille, T. (2022). Periodic/Aperiodic parameterization of transient oscillations (PAPTO)–Implications for healthy ageing. *NeuroImage*, *251*, 118974. https://doi.org/10.1016/j.neuroimage.2022.118974

Brunner, C., Billinger, M., Seeber, M., Mullen, T. R., & Makeig, S. (2016). Volume Conduction Influences Scalp-Based Connectivity Estimates. *Frontiers in Computational Neuroscience*, *10*. https://doi.org/10.3389/fncom.2016.00121

Bruns, A. (2004). Fourier-, Hilbert- and wavelet-based signal analysis: Are they really different approaches? *Journal of Neuroscience Methods*, *137*(2), 321–332. https://doi.org/10.1016/j.jneumeth.2004.03.002

Buzsáki, G., & Draguhn, A. (2004). Neuronal Oscillations in Cortical Networks. *Science*, *304*(5679), 1926–1929. https://doi.org/10.1126/science.1099745

Buzsáki, G., & Watson, B. O. (2012). Brain rhythms and neural syntax: Implications for efficient coding of cognitive content and neuropsychiatric disease. *Dialogues in Clinical Neuroscience*, *14*(4), 345–367. https://doi.org/10.31887/DCNS.2012.14.4/gbuzsaki

Cannon, J., McCarthy, M. M., Lee, S., Lee, J., Börgers, C., Whittington, M. A., & Kopell, N. (2014). Neurosystems: Brain rhythms and cognitive processing. *European Journal of Neuroscience*, *39*(5), 705–719. https://doi.org/10.1111/ejn.12453

Capilla, A., Arana, L., García-Huéscar, M., Melcón, M., Gross, J., & Campo, P. (2022). The natural frequencies of the resting human brain: An MEG-based atlas. *NeuroImage*, *258*, 119373. https://doi.org/10.1016/j.neuroimage.2022.119373

Caplan, J. B., Madsen, J. R., Raghavachari, S., & Kahana, M. J. (2001). Distinct Patterns of Brain Oscillations Underlie Two Basic Parameters of Human Maze Learning. *Journal of Neurophysiology*, *86*(1), 368–380. https://doi.org/10.1152/jn.2001.86.1.368

Cohen, M. X. (2017). Where Does EEG Come From and What Does It Mean? *Trends in Neurosciences*, *40*(4), 208–218. https://doi.org/10.1016/j.tins.2017.02.004

Donoghue, T. (2024). *A systematic review of aperiodic neural activity in clinical investigations*. Psychiatry and Clinical Psychology. https://doi.org/10.1101/2024.10.14.24314925

Donoghue, T., Haller, M., Peterson, E. J., Varma, P., Sebastian, P., Gao, R., Noto, T., Lara, A. H., Wallis, J. D., Knight, R. T., Shestyuk, A., & Voytek, B. (2020). Parameterizing neural power spectra into periodic and aperiodic components. *Nature Neuroscience*, *23*(12), 1655–1665. https://doi.org/10.1038/s41593-020-00744-x

Donoghue, T., Schaworonkow, N., & Voytek, B. (2022). Methodological considerations for studying neural oscillations. *European Journal of Neuroscience*, *55*(11–12), 3502–3527. https://doi.org/10.1111/ejn.15361

Fransen, A. M. M., Van Ede, F., & Maris, E. (2015). Identifying neuronal oscillations using rhythmicity. *NeuroImage*, *118*, 256–267. https://doi.org/10.1016/j.neuroimage.2015.06.003

Fries, P. (2015). Rhythms for Cognition: Communication through Coherence. *Neuron*, *88*(1), 220–235. https://doi.org/10.1016/j.neuron.2015.09.034

Gao, R., Peterson, E. J., & Voytek, B. (2017). Inferring synaptic excitation/inhibition balance from field potentials. *NeuroImage*, *158*, 70–78. https://doi.org/10.1016/j.neuroimage.2017.06.078

Gross, J. (2014). Analytical methods and experimental approaches for electrophysiological studies of brain oscillations. *Journal of Neuroscience Methods*, *228*, 57–66. https://doi.org/10.1016/j.jneumeth.2014.03.007

Gyurkovics, M., Clements, G. M., Low, K. A., Fabiani, M., & Gratton, G. (2022). Stimulus-Induced Changes in 1/ *f* -like Background Activity in EEG. *The Journal of Neuroscience*, *42*(37), 7144–7151. https://doi.org/10.1523/JNEUROSCI.0414-22.2022

He, B. J. (2014). Scale-free brain activity: Past, present, and future. *Trends in Cognitive Sciences*, *18*(9), 480–487. https://doi.org/10.1016/j.tics.2014.04.003

Helfrich, R. F., Fiebelkorn, I. C., Szczepanski, S. M., Lin, J. J., Parvizi, J., Knight, R. T., & Kastner, S. (2018). Neural Mechanisms of Sustained Attention Are Rhythmic. *Neuron*, *99*(4), 854-865.e5. https://doi.org/10.1016/j.neuron.2018.07.032

Herweg, N. A., Solomon, E. A., & Kahana, M. J. (2020). Theta Oscillations in Human Memory. *Trends in Cognitive Sciences*, *24*(3), 208–227. https://doi.org/10.1016/j.tics.2019.12.006

Izhikevich, E. M., Desai, N. S., Walcott, E. C., & Hoppensteadt, F. C. (2003). Bursts as a unit of neural information: Selective communication via resonance. *Trends in Neurosciences*, *26*(3), 161–167. https://doi.org/10.1016/S0166-2236(03)00034-1

Jackson, A. F., & Bolger, D. J. (2014). The neurophysiological bases of EEG and EEG measurement: A review for the rest of us. *Psychophysiology*, *51*(11), 1061–1071. https://doi.org/10.1111/psyp.12283

Jones, S. R. (2016). When brain rhythms aren't 'rhythmic': Implication for their mechanisms and meaning. *Current Opinion in Neurobiology*, *40*, 72–80. https://doi.org/10.1016/j.conb.2016.06.010

Jonmohamadi, Y., Poudel, G., Innes, C., Weiss, D., Krueger, R., & Jones, R. (2014). Comparison of beamformers for EEG source signal reconstruction. *Biomedical Signal Processing and Control*, *14*, 175–188. https://doi.org/10.1016/j.bspc.2014.07.014

Kalamangalam, G. P., Long, S., & Chelaru, M. I. (2020). A neurophysiological brain map: Spectral parameterization of the human intracranial electroencephalogram. *Clinical Neurophysiology*, *131*(3), 665–675. https://doi.org/10.1016/j.clinph.2019.11.061

Keitel, A., & Gross, J. (2016). Individual Human Brain Areas Can Be Identified from Their Characteristic Spectral Activation Fingerprints. *PLOS Biology*, *14*(6), e1002498. https://doi.org/10.1371/journal.pbio.1002498

Kosciessa, J. Q., Grandy, T. H., Garrett, D. D., & Werkle-Bergner, M. (2020). Single-trial characterization of neural rhythms: Potential and challenges. *NeuroImage*, *206*, 116331. https://doi.org/10.1016/j.neuroimage.2019.116331

Lega, B. C., Jacobs, J., & Kahana, M. (2012). Human hippocampal theta oscillations and the formation of episodic memories. *Hippocampus*, *22*(4), 748–761. https://doi.org/10.1002/hipo.20937

Lopes da Silva, F. (2013). EEG and MEG: Relevance to Neuroscience. *Neuron*, *80*(5), 1112–1128. https://doi.org/10.1016/j.neuron.2013.10.017

Mellem, M. S., Wohltjen, S., Gotts, S. J., Ghuman, A. S., & Martin, A. (2017). Intrinsic frequency biases and profiles across human cortex. *Journal of Neurophysiology*, *118*(5), 2853–2864. https://doi.org/10.1152/jn.00061.2017

Niso, G., Rogers, C., Moreau, J. T., Chen, L.-Y., Madjar, C., Das, S., Bock, E., Tadel, F., Evans, A. C., Jolicoeur, P., & Baillet, S. (2016). OMEGA: The Open MEG Archive. *NeuroImage*, *124*, 1182–1187. https://doi.org/10.1016/j.neuroimage.2015.04.028

Noah, S., Powell, T., Khodayari, N., Olivan, D., Ding, M., & Mangun, G. R. (2020). Neural Mechanisms of Attentional Control for Objects: Decoding EEG Alpha When Anticipating Faces, Scenes,and Tools. *The Journal of Neuroscience*, *40*(25), 4913–4924. https://doi.org/10.1523/JNEUROSCI.2685-19.2020

Nolte, G. (2003). The magnetic lead field theorem in the quasi-static approximation and its use for magnetoencephalography forward calculation in realistic volume conductors. *Physics in Medicine and Biology*, *48*(22), 3637–3652. https://doi.org/10.1088/0031-9155/48/22/002

O'Neill, G. C., Barratt, E. L., Hunt, B. A. E., Tewarie, P. K., & Brookes, M. J. (2015). Measuring electrophysiological connectivity by power envelope correlation: A technical review on MEG methods. *Physics in Medicine and Biology*, *60*(21), R271–R295. https://doi.org/10.1088/0031-9155/60/21/R271

Oostenveld, R., Fries, P., Maris, E., & Schoffelen, J.-M. (2011). FieldTrip: Open Source Software for Advanced Analysis of MEG, EEG, and Invasive Electrophysiological Data. *Computational Intelligence and Neuroscience*, *2011*, 1–9. https://doi.org/10.1155/2011/156869

Palva, J. M., & Palva, S. (2018). Functional integration across oscillation frequencies by cross-frequency phase synchronization. *European Journal of Neuroscience*, *48*(7), 2399–2406. https://doi.org/10.1111/ejn.13767

Quinn, A. J., Van Ede, F., Brookes, M. J., Heideman, S. G., Nowak, M., Seedat, Z. A., Vidaurre, D., Zich, C., Nobre, A. C., & Woolrich, M. W. (2019). Unpacking Transient Event Dynamics in Electrophysiological Power Spectra. *Brain Topography*, *32*(6), 1020–1034. https://doi.org/10.1007/s10548-019-00745-5

Seymour, R. A., Alexander, N., & Maguire, E. A. (2022). Robust estimation of 1/f activity improves oscillatory burst detection. *European Journal of Neuroscience*, *56*(10), 5836–5852. https://doi.org/10.1111/ejn.15829

Shapira Lots, I., Zeev-Wolf, M., Harpaz, Y., & Abeles, M. (2016). Source localization scale correction for Beamformer analysis. *Journal of Neuroscience Methods*, *273*, 10–19. https://doi.org/10.1016/j.jneumeth.2016.07.013

Shin, H., Law, R., Tsutsui, S., Moore, C. I., & Jones, S. R. (2017). The rate of transient beta frequency events predicts behavior across tasks and species. *eLife*, *6*, e29086. https://doi.org/10.7554/eLife.29086

The MathWorks Inc. (2024). *MATLAB* (Version 24.2.0.2740171 (R2024b)) [Computer software]. The MathWorks Inc. https://www.mathworks.com

Tzourio-Mazoyer, N., Landeau, B., Papathanassiou, D., Crivello, F., Etard, O., Delcroix, N., Mazoyer, B., & Joliot, M. (2002). Automated Anatomical Labeling of Activations in SPM Using a Macroscopic Anatomical Parcellation of the MNI MRI Single-Subject Brain. *NeuroImage*, *15*(1), 273–289. https://doi.org/10.1006/nimg.2001.0978

Van Bree, S., Levenstein, D., Krause, M., Voytek, B., & Gao, R. (2024). *Decoupling Measurements and Processes: On the Epiphenomenon Debate Surrounding Brain Oscillations in Field Potentials*. https://doi.org/10.31234/osf.io/knjfw

Van Den Broek, S. P., Reinders, F., Donderwinkel, M., & Peters, M. J. (1998). Volume conduction effects in EEG and MEG. *Electroencephalography and Clinical Neurophysiology*, *106*(6), 522–534. https://doi.org/10.1016/S0013-4694(97)00147-8

Van Ede, F., Quinn, A. J., Woolrich, M. W., & Nobre, A. C. (2018). Neural Oscillations: Sustained Rhythms or Transient Burst-Events? *Trends in Neurosciences*, *41*(7), 415–417. https://doi.org/10.1016/j.tins.2018.04.004

Van Veen, B. D., Van Drongelen, W., Yuchtman, M., & Suzuki, A. (1997). Localization of brain electrical activity via linearly constrained minimum variance spatial filtering. *IEEE Transactions on Biomedical Engineering*, *44*(9), 867–880. https://doi.org/10.1109/10.623056

Vidaurre, D., Quinn, A. J., Baker, A. P., Dupret, D., Tejero-Cantero, A., & Woolrich, M. W. (2016). Spectrally resolved fast transient brain states in electrophysiological data. *NeuroImage*, *126*, 81–95. https://doi.org/10.1016/j.neuroimage.2015.11.047

Vinck, M., Uran, C., Spyropoulos, G., Onorato, I., Broggini, A. C., Schneider, M., & Canales-Johnson, A. (2023). Principles of large-scale neural interactions. *Neuron*, *111*(7), 987–1002. https://doi.org/10.1016/j.neuron.2023.03.015

Westner, B. U., Kujala, J., Gross, J., & Schoffelen, J.-M. (2023). *Towards a more robust non-invasive assessment of functional connectivity* [Preprint]. Neuroscience. https://doi.org/10.1101/2023.02.06.527279

Whitten, T. A., Hughes, A. M., Dickson, C. T., & Caplan, J. B. (2011). A better oscillation detection method robustly extracts EEG rhythms across brain state changes: The human alpha rhythm as a test case. *NeuroImage*, *54*(2), 860–874. https://doi.org/10.1016/j.neuroimage.2010.08.064